Immunity
Article

The DNA-Binding Protein CTCF Limits Proximal Vκ Recombination and Restricts κ Enhancer Interactions to the Immunoglobulin κ Light Chain Locus

Claudia Ribeiro de Almeida,[1] Ralph Stadhouders,[2] Marjolein J.W. de Bruijn,[1] Ingrid M. Bergen,[1] Supat Thongjuea,[5] Boris Lenhard,[5,6] Wilfred van IJcken,[3] Frank Grosveld,[2,4] Niels Galjart,[2] Eric Soler,[2,4] and Rudi W. Hendriks[1,*]
[1]Department of Pulmonary Medicine
[2]Department of Cell Biology and Genetics
[3]Center for Biomics
[4]The Cancer Genomics Center
Erasmus MC Rotterdam, P.O. Box 2040, 3000 CA Rotterdam, The Netherlands
[5]Computational Biology Unit— Bergen Center for Computational Science and Sars Centre for Marine Molecular Biology
[6]Department of Biology
University of Bergen, Thormøhlensgate 55, N-5008, Bergen, Norway
*Correspondence: r.hendriks@erasmusmc.nl
DOI 10.1016/j.immuni.2011.07.014

SUMMARY

Regulation of immunoglobulin (Ig) V(D)J gene rearrangement is dependent on higher-order chromatin organization. Here, we studied the in vivo function of the DNA-binding zinc-finger protein CTCF, which regulates interactions between enhancers and promoters. By conditional deletion of the *Ctcf* gene in the B cell lineage, we demonstrate that loss of CTCF allowed Ig heavy chain recombination, but pre-B cell proliferation and differentiation was severely impaired. In the absence of CTCF, the Igκ light chain locus showed increased proximal and reduced distal Vκ usage. This was associated with enhanced proximal Vκ and reduced Jκ germline transcription. Chromosome conformation capture experiments demonstrated that CTCF limits interactions of the Igκ enhancers with the proximal V_κ gene region and prevents inappropriate interactions between these strong enhancers and elements outside the Igκ locus. Thus, although Ig gene recombination can occur in the absence of CTCF, it is a critical factor determining Vκ segment choice for recombination.

INTRODUCTION

Antigen receptor diversity of lymphocytes is achieved through recombinase activating gene (RAG)-mediated DNA recombination of V (variable), D (diversity), and J (joining) gene segments at the immunoglobulin (Ig) and T cell receptor (Tcr) loci in B and T lymphocytes, respectively (Jung and Alt, 2004; Schlissel, 2003). The process of V(D)J recombination is regulated at three different levels: lineage specificity, temporal order within a lineage, and allelic exclusion.

B cells develop in the bone marrow (BM) through an orchestrated network of transcription factors and signaling pathways (Nutt and Kee, 2007). Ig heavy-chain (*Igh*) V(D)J recombination starts at the pre-pro-B cell stage with D_H-to-J_H rearrangement, which precedes V_H-to-DJ_H rearrangement in committed pro-B cells. Productive *Igh* rearrangement leads to Igμ H chain expression on the cell surface together with the surrogate light chain (SLC) components λ5 and VpreB as the precursor-B cell receptor (pre-BCR). Signals from the pre-BCR and the interleukin-7 receptor (IL-7R) drive proliferation of large pre-B cells (Hendriks and Middendorp, 2004; Herzog et al., 2009). Upon cessation of proliferation, pre-B cells undergo cellular differentiation and transit to the small pre-B cell stage where Ig κ or λ light-chain (*Igl*) V_L-to-J_L recombination is initiated (Herzog et al., 2009; Schlissel, 2003). Productive *Igl* rearrangement results in surface BCR expression and progression to immature B cells, which are checked for autoreactivity before they leave the BM.

Mechanisms regulating V(D)J recombination are complex and rely on developmental-stage specific changes in locus accessibility to the RAG-recombinase (Jhunjhunwala et al., 2009; Jung and Alt, 2004; Schlissel, 2003). They include subnuclear relocation, histone modifications, DNA demethylation, germline transcription, antisense intergenic transcription, and locus contraction mediated by looping of individual chromatin domains. Accessibility is controlled by *cis*-regulatory elements within the Ig loci, such as promoters, matrix attachment regions, silencers, and enhancers, where binding of cell type-specific transcription factors like Pax5, E2A, Ikaros, IRF4, or OBF-1 account for lineage- and developmental-stage specificity of V(D)J recombination (Jhunjhunwala et al., 2009; Jung and Alt, 2004; Schlissel, 2003). Pax5 and Ikaros were shown to be involved in *Igh* locus contraction and in their absence only the D_H proximal V_H genes recombine (Fuxa et al., 2004; Reynaud et al., 2008). Deletion of the transcription factor YY1 also prevented *Igh* locus contraction, resulting in severely reduced distal V_H rearrangement (Liu et al., 2007). These studies indicate that lineage-specific and ubiquitously expressed transcription factors cooperate to establish higher-order chromatin structures that facilitate long-range interactions required for V_H-DJ_H or V_κ-J_κ rearrangement (Jhunjhunwala et al., 2008; Jhunjhunwala et al., 2009).

One DNA-binding factor implicated in long-range interactions is the CCCTC-binding factor (CTCF), a ubiquitously expressed and highly conserved 11 zinc finger protein (Phillips and Corces, 2009). CTCF often controls specific interactions by preventing inappropriate communication between neighboring regulatory elements and/or independent chromatin domains, in a developmentally regulated fashion. Gene insulation mediated by CTCF may occur through the formation of chromatin loop domains, as shown for the imprinted H19-Igf2 locus, the mouse β-globin locus, and at boundaries of domains escaping inactivation on the inactive X chromosome (Splinter et al., 2006; reviewed in Phillips and Corces, 2009). In T helper 1 (Th1) cells, CTCF cooperates with the Th1 cell lineage-specific transcription factor T-bet for proper interferon-γ (IFN-γ) expression via regulation of chromatin looping (Sekimata et al., 2009). We recently showed that CTCF is also a critical regulator of cytokine genes at the Th2 cytokine locus (Ribeiro de Almeida et al., 2009).

A putative role for CTCF in Ig loci long-range interactions was highlighted by the recent mapping of CTCF-binding sites across the Ig loci (Degner et al., 2009; Ebert et al., 2011; Lucas et al., 2011). Two CTCF-binding sites in the *Igh* V_H-D_H intergenic region were implicated in the control of lineage-specific and ordered V(D)J recombination by separating the V_H and D_H regions into distinct chromatin domains (Featherstone et al., 2010; Giallourakis et al., 2010). CTCF sites flank recombination signal sequences (RSSs) for many *Igh* proximal V_H segments (Lucas et al., 2011). In the distal V_H region, CTCF and E2A were shown to interact with Pax5-activated intergenic repeat (PAIR) elements, which direct antisense transcription (Ebert et al., 2011). Recently, knockdown of CTCF resulted in a modest reduction in *Igh* locus contraction and increased antisense transcription throughout the D_H region and in distal V_H segments near PAIR elements (Degner et al., 2011).

Collectively, these data prompted us to investigate the in vivo function of CTCF in B cell development. Here we show that conditional *Ctcf* deletion in the B cell lineage still allowed for the generation of cytoplasmic Igμ expressing pre-B cells, although they were severely hampered in proliferation and cellular differentiation. For the *Igκ* locus, we found preferential recombination and increased germline transcription of proximal $V_κ$ gene segments. Chromosome conformation capture assays coupled to high-throughput sequencing (3C-Seq) (Soler et al., 2010) revealed that CTCF limits interactions of κ enhancers with proximal $V_κ$ genes and prevents inappropriate interactions between these strong enhancers and elements outside the *Igκ* locus.

RESULTS

Deletion of CTCF Ablates Early B Cell Development

To determine the function of CTCF in B cell development, we crossed *Ctcf* floxed mice (*Ctcf*$^{fl/fl}$) (Heath et al., 2008) with mb1-cre mice expressing Cre recombinase specifically in the B cell lineage (Hobeika et al., 2006). Flow cytometric analyses showed severely decreased proportions of B220$^+$CD19$^+$ B lineage cells in the BM of mb1-cre *Ctcf*$^{fl/fl}$ mice, when compared with wild-type (WT) controls (Figure 1A). Residual B-lineage cells were mainly intracellular Igμ$^-$ pro-B cells, although a detectable fraction expressed intracellular Igμ, indicating productive *Igh* rearrangement (Figures 1A and 1B). An almost complete block of early B cell development in mb1-cre *Ctcf*$^{fl/fl}$ BM was evidenced by the lack of CD2$^+$ small pre-B, immature B, and recirculating mature B cells (Figures 1A and 1B). B220$^+$CD19$^+$ cells were virtually absent in mb1-cre *Ctcf*$^{fl/fl}$ spleen or peritoneal cavity (Figure 1C). Crosses of mb1-cre *Ctcf*$^{fl/fl}$ mice with mice carrying the antiapoptotic Eμ-Bcl2 transgene (Strasser et al., 1991) demonstrated that the developmental block of CTCF-deficient pre-B cells could not be explained by defective survival only (see Figure S1 available online).

We used the *LacZ* reporter in the targeted *Ctcf* allele (Heath et al., 2008) to evaluate the efficiency of deletion (Figure S1). Consistent with previously reported highly efficient gene deletion at the earliest stages of B cell development with mb1-cre mice (Hobeika et al., 2006; Liu et al., 2007), *Ctcf* deletion occurred already at the pre-pro-B cell stage (fraction A) (Hardy et al., 1991) and was almost complete from the pro-B cell stage (fraction B) onward (Figure 1D). Accordingly, CTCF mRNA and protein were essentially undetectable in B220$^+$CD19$^+$ B lineage fractions purified from mb1-cre *Ctcf*$^{fl/fl}$ BM (Figures 1E and 1F).

These findings show that in mb1-cre *Ctcf*$^{fl/fl}$ mice CTCF expression is efficiently ablated in early stages of B cell development and that CTCF is essential beyond the pre-B cell stage.

Defective Pre-B Cell Proliferation and Differentiation in Mb1-Cre *Ctcf*$^{fl/fl}$ Mice

The pre-BCR acts as a checkpoint that monitors functional *Igh* rearrangement and induces, together with IL-7R signaling, clonal expansion and survival of Igμ$^+$ large pre-B cells. Upon cessation of proliferation, pre-BCR signals are additionally required for developmental progression of large into small pre-B cells (Hendriks and Middendorp, 2004; Herzog et al., 2009).

Flow cytometric analysis of Igμ$^+$ pre-B cells from mb1-cre *Ctcf*$^{fl/fl}$ mice showed reduced cell size, indicating defective proliferation (Figure 2A). Additionally, mb1-cre *Ctcf*$^{fl/fl}$ pro-B and large pre-B cells both showed decreased expression of IL-7R α chain by flow cytometry (Figure 2A) and RT-PCR (Figure S2C). To directly examine the cell cycle status of B-lineage cells in mb1-cre *Ctcf*$^{fl/fl}$ mice, we measured DNA content by propidium iodide staining. Although the proportions of cycling pro-B cells were similar, we observed a considerable reduction in the proportions of cycling large pre-B cells in mb1-cre *Ctcf*$^{fl/fl}$ mice, when compared with WT mice (~26% versus ~47%, respectively, Figure 2B). Subsequently, we determined the proliferation capacity in vivo by pulsing with a single dose of the thymidine analog 5-bromodeoxyuridine (BrdU), which is selectively incorporated into the DNA of cycling cells (Middendorp et al., 2002). Flow cytometric analysis revealed comparable proportions of BrdU$^+$ pro-B cells, but a ~50% reduction in the fractions of BrdU$^+$ large pre-B cells in mb1-cre *Ctcf*$^{fl/fl}$ mice, when compared with WT controls (Figure 2C).

Consistent with a strong pre-B cell arrest, the majority of B220$^+$CD19$^+$ cells in mb1-cre *Ctcf*$^{fl/fl}$ BM expressed the early pro-B cell-specific markers c-Kit, CD43, and the SLC component λ5 and failed to upregulate CD2, CD25, and MHC class II expression (Figure S2A). Quantitative RT-PCR analyses of purified B220$^+$CD19$^+$CD2$^-$ cells from WT and mb1-cre *Ctcf*$^{fl/fl}$ BM showed proper specification and commitment to the

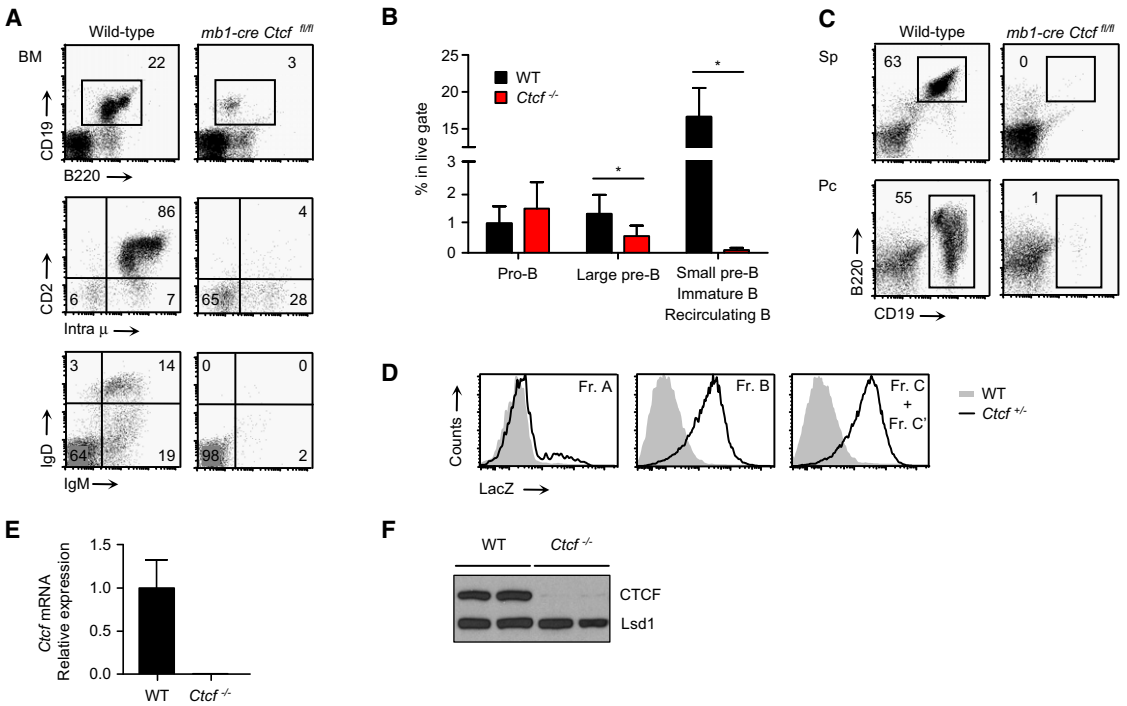

Figure 1. Impaired B Cell Development in Mb1-Cre *Ctcf*$^{fl/fl}$ Mice

(A) Flow cytometric analysis of WT and mb1-cre *Ctcf*$^{fl/fl}$ total BM cells for expression of B220 and CD19 (top). B220$^+$CD19$^+$ B cell fractions were gated and analyzed for intracellular Igμ-CD2 (middle) or IgM-IgD (bottom). Data are representative of 14–28 mice per genotype. Numbers in dot plots indicate the percentages of cells in each gate.

(B) Proportions of cells in live gate were calculated for pro-B (CD2$^-$ intracellular Igμ$^-$), large pre-B (CD2$^-$ intracellular Igμ$^+$) and total small pre-B, immature B, and recirculating mature B cell fractions (CD2$^+$ intracellular Igμ$^+$) in BM of WT and mb1-cre *Ctcf*$^{fl/fl}$ mice (mean and standard deviation [SD], *$p < 0.001$).

(C) CD19/B220 flow cytometry profiles of WT and mb1-cre *Ctcf*$^{fl/fl}$ spleen (Sp) and peritoneal cavity (PC) lymphoid fractions. Dot plots are representative of 6–7 mice per genotype.

(D) Flow cytometric *lacZ* expression analysis of BM cells of the indicated mice. Results are shown as histogram overlays within three subsets: fraction A (Lin$^-$B220$^+$CD19$^-$HSA$^{-/lo}$CD43$^+$), fraction B (CD19$^+$CD43$^+$BP-1$^-$HSA$^+$), and fraction C+C' (CD19$^+$CD43$^+$BP-1$^+$HSA$^{+/high}$).

(E and F) Purified B220$^+$CD19$^+$CD2$^-$ pro-B or large pre-B cells from BM of the indicated mice were analyzed by quantitative RT-PCR (E) or immunoblotting (F). *Ctcf* expression levels were normalized to the levels of *Gapdh*, whereby the values in WT cells were set to one (mean and SD, for 3 pools of 6–7 mice per genotype). Nuclear protein lysates were analyzed by immunoblotting for CTCF and Lsd1 as a protein loading control (2 pools of 6–7 mice per genotype). See also Figure S1.

B cell fate, given that CTCF-deficient cells still expressed the early B lineage genes *Tcfe2a*, *Ebf1*, *Pax5*, *Il7ra*, *Cd79a*, and *Cd79b*, albeit often at slightly reduced levels (Figure S2A). For genes that are normally up or downregulated upon pre-BCR signaling (*Igll1*, *Vpreb1 Irf4*, *Ikzf1*) expression levels in CTCF-deficient B220$^+$CD19$^+$CD2$^-$ cells were between those in *Rag1*$^{-/-}$ and WT fractions (Figure S2A), indicating that pre-BCR signaling was not completely abrogated in the absence of CTCF.

Genome-wide expression profiling of purified and CTCF-deficient CD2$^-$ B220$^+$CD19$^+$ fractions (containing pro-B and pre-B cells) revealed that 174 genes were differently expressed. Approximately 50% of these genes demonstrated a pro-B cell signature for CTCF-deficient B cell precursors, given that these genes were also differentially expressed between *Rag1*$^{-/-}$ pro-B cells and V_H81X *Igh* transgenic *Rag1*$^{-/-}$ pre-B cells (Figure 2D; Table S1). Other genes were upregulated in the absence of CTCF, irrespective of B cell differentiation stage (Figure 2E; Table S2).

In summary, our findings show that CTCF-deficient cytoplasmic Igμ$^+$ pre-B cells manifested defective proliferation and a severe block of cellular differentiation.

Igh V(D)J Rearrangement Occurs in CTCF-Deficient Pro-B Cells

The presence of intracellular Igμ$^+$ pre-B cells in mb1-cre *Ctcf*$^{fl/fl}$ BM indicated successful *Igh* gene rearrangement in the absence of CTCF. In addition, RT-PCR analysis revealed normal levels of V_HJ558, V_H7183, and Iμ germline transcripts in B220$^+$CD19$^+$CD2$^-$ fractions from mb1-cre *Ctcf*$^{fl/fl}$ mice, suggesting unaltered *Igh* locus accessibility (Schlissel, 2003) (Figures S2D and S2E). We used quantitative RT-PCR to compare V_H family usage (Fuxa et al., 2004) in purified B220$^+$CD19$^+$CD2$^-$ fractions from WT and mb1-cre *Ctcf*$^{fl/fl}$ mice. We included μMT mice harboring a targeted deletion of the Igμ membrane exon (Kitamura et al., 1991) as a control because they parallel CTCF-deficient mice in that pre-BCR-induced proliferative expansion and concomitant selection for particular V_H segments in the context of the

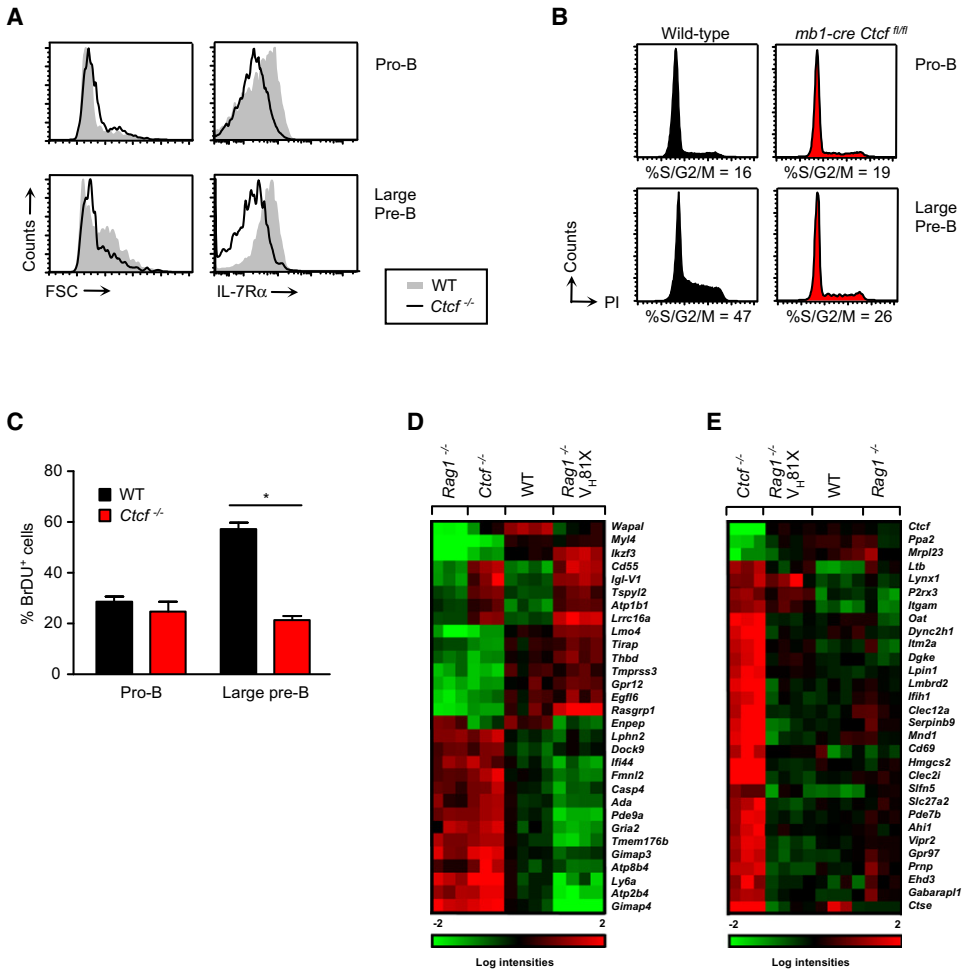

Figure 2. Defective Pre-B Cell Proliferation and Differentiation in Mb1-Cre *Ctcf*$^{fl/fl}$ Mice

(A) Flow cytometric analysis of WT and mb1-cre *Ctcf*$^{fl/fl}$ B220^{+}CD19^{+} pro-B cells (CD2^{-} intracellular Igμ^{-}) and large pre-B cells (CD2^{-} intracellular Igμ^{+}) for cell size (forward side scatter [FSC]) and IL-7Rα. Results are displayed as histogram overlays (4–6 mice per genotype).

(B) Propidium iodide (PI) cell cycle analysis of B220^{+}CD19^{+} pro-B cells (CD2^{-} intracellular Igμ^{-}) and large pre-B cells (CD2^{-}intracellular Igμ^{+}) purified from WT and mb1-cre *Ctcf*$^{fl/fl}$ BM. Percentages of cells in cycle (S/G2/M; >2N DNA content) are shown (representative of two mice per genotype).

(C) In vivo proliferation analysis of WT and mb1-cre *Ctcf* $^{fl/fl}$ B220^{+}CD19^{+} pro-B cells (CD2^{-} intracellular Igμ^{-}) and large pre-B cells (CD2^{-} intracellular Igμ^{+}). Mice were i.p. injected with a single dose of BrdU and after 4 hr, the percentages of BrdU^{+} cells were determined by flow cytometry (mean values and SD for 3–4 mice per genotype; *$p < 0.001$).

(D and E) DNA microarray analysis of total mRNA from purified B220^{+}CD19^{+}CD2^{-} pro-B/large pre-B cell fractions in WT and mb1-cre *Ctcf*$^{fl/fl}$ mice. Genes differentially expressed between the two genotypes were subdivided into two groups: genes in which expression did (D) or did not differ (E) between control *Rag1*$^{-/-}$ pro-B cell and V_H81X *Rag1*$^{-/-}$ pre-B cell fractions. Heatmaps for the 30 genes with highest fold change in expression between WT and mb1-cre *Ctcf*$^{fl/fl}$ B cell progenitors are shown (for complete gene lists, see Tables S1 and S2). On the bottom is the logarithmic quantitative scale for gene expression (3–4 pools of 3–7 mice per genotype). See also Figure S2.

pre-BCR (ten Boekel et al., 1997) is absent. We found that in the absence of CTCF proximal (V_H7183) as well as distal (V_HJ558) gene segments were used, whereby their relative usage was close to that of μMT mice (Figure S2F). Thus, *Igh* gene recombination, even to distal V_H gene segments, occurred in CTCF-deficient pro-B cells.

A Productively Rearranged *Igh* Transgene Allows CTCF-Deficient Cells to Develop beyond the Pre-B Cell Stage

The nearly complete developmental block observed in mb1-cre *Ctcf*$^{fl/fl}$ mice precluded the analysis of CTCF function past the pre-B cell stage. However, upon introduction of the functionally pre-rearranged Igμ transgene V_H81X (Martin et al., 1997), B cell differentiation was partially rescued: we found substantial populations of CD2^{+} and surface IgM^{+} B-lineage cells in V_H81X mb1-cre *Ctcf*$^{fl/fl}$ BM (Figure 3A). Although the V_H81X transgene did not appear to rescue the proliferation defect of CTCF-deficient large pre-B cells (Figures S3A–S3C), the proportions of large pre-B cells in vivo were not significantly different between V_H81X and V_H81X mb1-cre *Ctcf*$^{fl/fl}$ BM (Figure 3B). Furthermore, we observed a partial correction of the expression profiles of the developmentally regulated markers c-Kit, CD43, CD2, CD25, MHC class II,

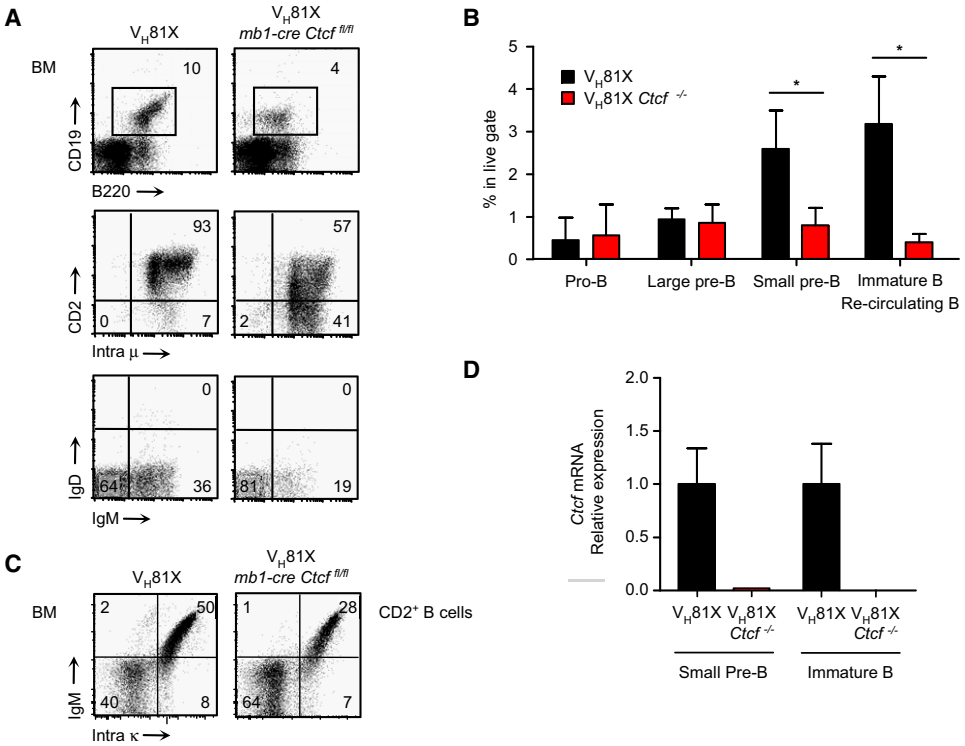

Figure 3. B Cell Development in V_H81X Transgenic Mb1-Cre *Ctcf*$^{fl/fl}$ Mice

(A) Flow cytometric analysis of V_H81X and V_H81X mb1-cre *Ctcf*$^{fl/fl}$ BM cells for the expression of B220/CD19 (top). Total B220$^+$CD19$^+$ B cell fractions were gated and analyzed for expression of intracellular Igμ/CD2 (middle) or IgM/IgD (bottom). Data are representative of 7–14 mice per genotype. Numbers in dot plots indicate the percentages of cells in each gate.

(B) Proportions of cells in live gate were calculated for pro-B (CD2$^-$ intracellular Igμ$^-$), large pre-B (CD2$^-$ intracellular Igμ$^+$), small pre-B (CD2$^+$IgM$^-$) and immature B/recirculating mature B cell (CD2$^+$IgM$^+$) fractions in the BM of V_H81X and V_H81X mb1-cre *Ctcf*$^{fl/fl}$ mice (mean values and SD, *$p < 0.001$).

(C) Flow cytometric analysis of gated B220$^+$CD19$^+$CD2$^+$ cells from V_H81X and V_H81X mb1-cre *Ctcf*$^{fl/fl}$ BM for the expression of IgM/ intracellular Igκ. Data are representative of 13–14 mice per genotype.

(D) Total RNA isolated from purified B220$^+$CD19$^+$CD2$^+$ IgM$^-$ (small pre-B cells) and IgM$^+$ (immature/recirculating mature B cells) populations from V_H81X and V_H81X mb1-cre *Ctcf*$^{fl/fl}$ BM was analyzed by quantitative RT-PCR for *Ctcf* expression. *Ctcf* expression levels were normalized to the levels of *Gapdh* mRNA, whereby the values in V_H81X cells were set to one (mean values and SD, for three pools of six to seven mice per genotype). See also Figure S3.

and λ5 (Figure S3D). V_H81X mb1-cre *Ctcf*$^{fl/fl}$ BM manifested decreased proportions of CD2$^+$ small pre-B cells, immature and recirculating mature IgM$^+$ B cells, when compared with V_H81X controls (Figures 3A and 3B). However, intracellular Igκ L chain expression in surface IgM$^-$ small pre-B cells and IgM$^+$ immature B cells was quite similar in the two groups of mice (Figure 3C).

The reduced size of the small pre-B and immature B cell population in V_H81X mb-1-cre *Ctcf*$^{fl/fl}$ BM prompted us to investigate the kinetics of the developmental progression of pre-B cells in vivo by BrdU injection. We found only a minor developmental delay of ~1.5 hr in CTCF-deficient V_H81X Igκ$^+$ immature B cells (~12 hr), compared with V_H81X controls (~10.5 hr, Figures S3E and S3F). B220^{low}CD19$^+$ B cells were detected in the spleen at low numbers but were absent in peritoneal cavity of V_H81X mb1-cre *Ctcf*$^{fl/fl}$ mice (Figure S3G). As assessed by quantitative RT-PCR, CTCF mRNA was strongly reduced in B220$^+$CD19$^+$ subsets purified from V_H81X mb1-cre *Ctcf* $^{fl/fl}$ BM (Figure 3D).

Thus, expression of the V_H81X transgene allowed significant differentiation of CTCF-deficient cells beyond the large pre-B cell stage.

Increased Proximal $V_κ$ Gene and Reduced $J_κ$ Germline Transcription in the Absence of CTCF

In small pre-B cells, successful *Igl* V-to-J recombination requires that these gene segments are accessible to the recombination machinery, which is reflected by germline transcription (Schlissel and Baltimore, 1989) (Schlissel, 2003). We determined *Igκ* and *Igλ* locus germline transcription in sorted CD2$^+$ small pre-B cell fractions by quantitative RT-PCR (Düber et al., 2003; Inlay et al., 2006). We found remarkably increased germline transcription of the proximal $V_κ$ gene segment $V_κ$3-7 in Ctcf-deficient V_H81X small pre-B cells, compared with V_H81X controls (Figure 4A). Germline transcription of more distal $V_κ$ gene segments was only slightly increased or not significantly different. In contrast, germline transcripts initiating from promoters located upstream of $J_κ$ ($κ^0$0.8, $κ^0$1.1) (Grawunder et al., 1995) were substantially reduced in the absence of CTCF (Figure 4A). Germline transcription from the $J_λ$1 and $J_λ$3 clusters (λ1° and λ3°, respectively (Engel et al., 1999) were increased, whereas $V_λ$1,2 (Düber et al., 2003) and λ2° germline transcripts were not affected (Figure 4A).

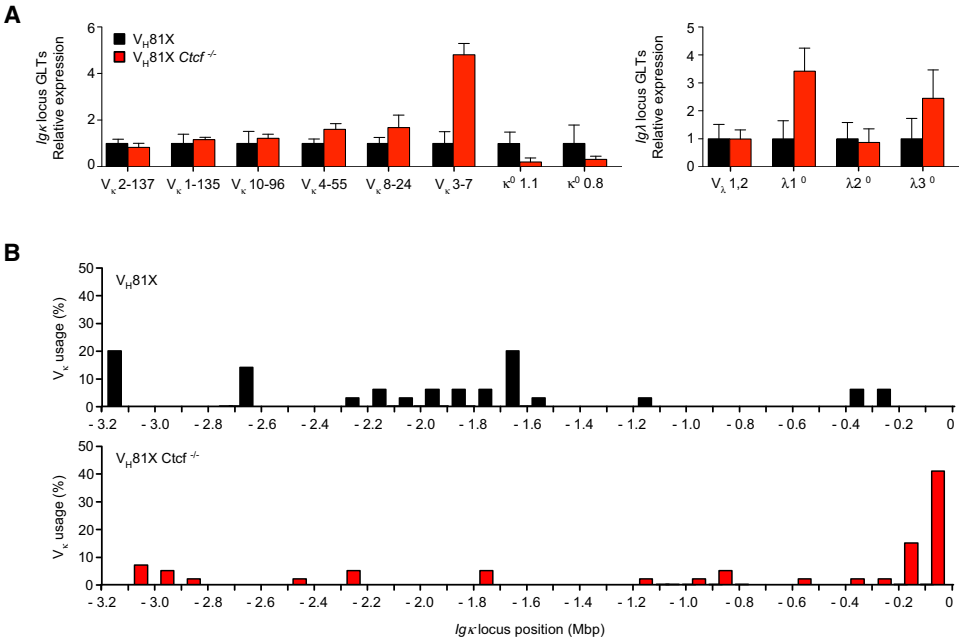

Figure 4. Proximal V_κ Usage in V_H81X Transgenic Mb1-Cre *Ctcf*$^{fl/fl}$ (pre-)B Cells

(A) Quantitative RT-PCR analysis for *Igκ* and *Igλ* locus germline transcription in purified B220$^+$CD19$^+$CD2$^+$IgM$^-$ small pre-B cell populations from V_H81X and V_H81X mb1-cre *Ctcf*$^{fl/fl}$ BM. Expression levels of different germline transcripts (GLTs) were normalized to the levels of *Gapdh*, whereby the values in V_H81X small pre-B cells were set to one. Data represent V_H81X mb1-cre *Ctcf* $^{fl/fl}$ mean values and SD for three independent pools of three to five mice.

(B) DNA sequencing analysis of V_κ gene segment usage of nonproductive alleles from B220$^+$CD19$^+$CD2$^+$IgM$^-$ small pre-B cell and B220$^+$CD19$^+$CD2$^+$IgM$^+$ (im) mature B cell populations purified from V_H81X and V_H81X mb1-cre *Ctcf*$^{fl/fl}$ BM. Genomic DNA was isolated and used for PCR amplification of V_κ-J_κ2 recombination products, which were further cloned and analyzed by DNA sequencing. Data represent relative frequency of V_κ usage per 0.2 Mbp intervals in the *Igκ* locus. A schematic representation of the *Igκ* locus (top) shows the location of V_κ genes in which germline transcription was analyzed in (A). Data are from three independent pools of three to five mice per genotype (number of sequences analyzed: 35 sequences for V_H81X B cells; 41 sequences for V_H81X mb1-cre *Ctcf* $^{fl/fl}$ B cells). See also Figure S4.

In conclusion, loss of CTCF resulted in increased germline transcription of the V_κ proximal region and reduced κ^0 germline transcription over the J_κ region in pre-B cells.

Proximal V_κ Usage in V_H81X Transgenic CTCF-Deficient B Cells

Next, we analyzed V_κ gene usage by DNA sequencing of V_κ-J_κ recombination products from purified pre-B and B cells. To exclude repertoire effects of BCR-mediated selection, we first focused on nonproductively rearranged alleles from control (n = 35) and CTCF-deficient (n = 41) V_H81X (pre-)B cells. We calculated V_κ gene usage for 100 kb intervals within the *Igκ* locus. In control V_H81X (pre-)B cells, V_κ usage was diverse and for > 80% directed to the middle and distal regions of the *Igκ* locus (Figure 4B). Remarkably, in CTCF-deficient V_H81X (pre-) B cells, >50% of all V_κ segments used were located in the most proximal ~200 kb region, exclusively containing members of the V_κ3 family. Importantly, this region was not used in control V_H81X (pre-)B cells (Figure 4B).

It is conceivable that CTCF indirectly controls *Igκ* locus recombination. CTCF might affect survival and thereby receptor editing, the process of ongoing Ig L chain recombination that serves to replace autoreactive BCR specificities. However, when we excluded cells that had performed receptor editing by analyzing V_κ gene usage in J_κ1 recombination products only, we still observed increased V_κ3 usage in CTCF-deficient cells (24 out of 31, as compared with 0/14 in WT cells). We also found that in the absence of CTCF both inversional and deletional Ig κ recombination events occurred (Figure S4A). Thus, reduced receptor editing or specific defects in either inversional or deletional recombination cannot explain the increased V_κ3 usage in the absence of CTCF. It remained possible that CTCF indirectly controls *Igκ* locus recombination through regulation of other transcription factors, but we found that loss of CTCF did not significantly affect the expression of nuclear proteins implicated in *Igκ* locus recombination (Schlissel, 2003), including *Tcfe2a*, *Id3*, *Ikzf3*,, *Irf4*, *Irf8*, *Pou2af1*, *Ccdn3*, *Rag1*, and *Rag2* (Figure S4B).

Taken together, these findings show that in the absence of CTCF V_κ-J_κ recombination activity is preferentially targeted to V_κ3, consistent with the observed increased germline transcription over the V_κ proximal region.

BCR-Mediated Selection Still Occurs in CTCF-Deficient Immature B Cells

Detailed analysis of the *Igκ* locus 1.0 Mbp proximal region showed that in the absence of CTCF V_κ usage in nonproductive rearrangements was highly restricted to the V_κ3 family, whereby V_κ3-4 was dominant (Figure 5A). Analysis of V_κ-to-J_κ1 rearrangements yielded a similar distribution, showing that the observed

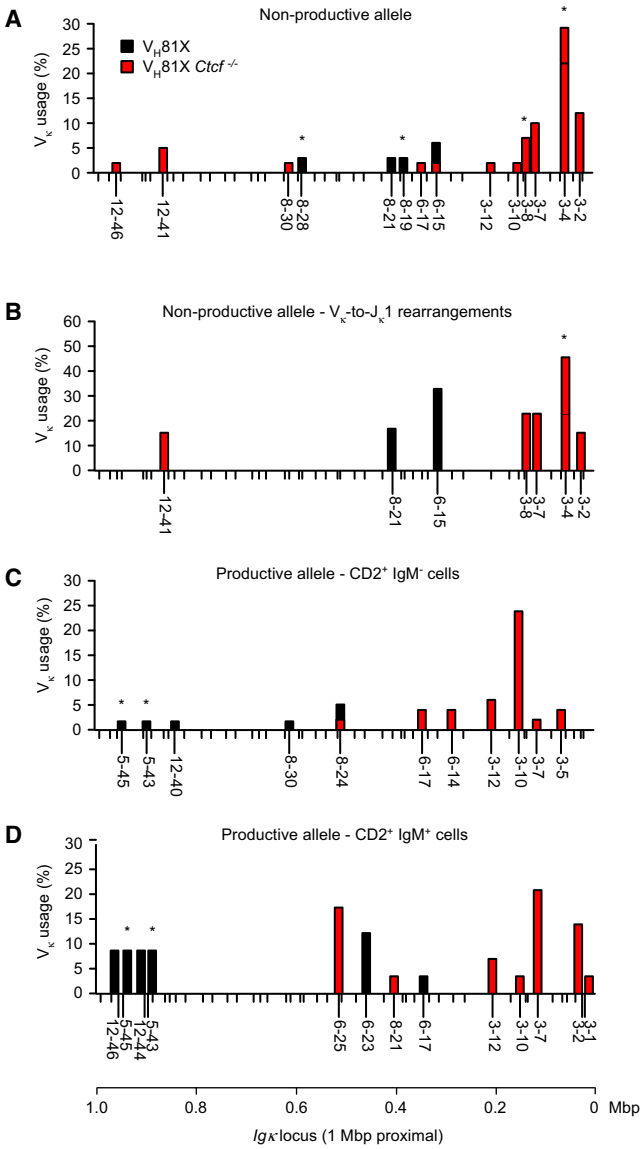

Figure 5. Proximal V_κ Repertoire in V_H81X Transgenic mb1-cre *Ctcf*$^{fl/fl}$ (pre-)B Cells

DNA sequencing analysis of V_κ gene segments used in total nonproductive *Igκ* alleles (A), nonproductive V_κ-to-J_κ1 alleles (B), productive *Igκ* alleles from B220$^+$CD19$^+$CD2$^+$IgM$^-$ small pre-B cells (C), and B220$^+$CD19$^+$CD2$^+$IgM$^+$ (im) mature B cells (D) purified from V_H81X and V_H81X mb1-cre *Ctcf*$^{fl/fl}$ BM. Data represent relative frequency of individual V_κ gene segments used for the proximal 1 Mbp region of the *Igκ* locus. In each panel, the x axis shows the location of various V_κ gene segments. Collective data are from three independent pools of three to five mice per genotype (number of sequences analyzed for V_H81X and for V_H81X mb1-cre *Ctcf*$^{fl/fl}$ mice are for nonproductive alleles: 35 and 41, respectively; for productive alleles in IgM$^-$ small pre-B: 32 and 30; and for productive alleles in IgM$^+$ B cells: 36 and 30. Some DNA sequences cannot exclusively be assigned to a single V_κ gene segment (see 8-19/8-28, 3-4/ 3-8 and 5-43/5-45 (marked with an asterisk).

differences between control and CTCF-deficient alleles were not dependent on receptor editing events (Figure 5B). In addition, productive alleles in CTCF-deficient cells manifested preferential V_κ3 usage (32/60 alelles, versus 0/60 in WT controls). Hereby V_κ3-10 and V_κ3-7 segments were predominantly used in surface IgM$^-$ small pre-B cells and surface IgM$^+$ B cells, respectively (Figures 5C and 5D). The finding that relative frequencies of individual V_κ3 family members differed considerably between productive and unproductive Igκ alleles indicates that BCR-mediated selection still occurred in the absence of CTCF. Moreover, the observed increased usage of V_κ3 in the absence of CTCF affected all V_κ3 family members.

V_κ Usage Is Correlated with CTCF-Binding Sites in the *Igκ* Locus

Next, we identified CTCF-binding sites in the *Igκ* locus in cultured primary pre-B cells using chromatin immunoprecipitation coupled to high-throughput sequencing (ChIP-Seq) (Figure 6A). We identified predominant CTCF binding at the 5′ and 3′ boundaries of *Igκ* locus, as well as at the SIS (silencer in intervening sequence) recombination silencer element residing in the V_κ-J_κ region (Liu et al., 2006), in agreement with reported findings (Degner et al., 2009). The SIS element has been shown to negatively regulate rearrangement and to specify targeting to centromeric heterochromatin (Liu et al., 2006). In contrast to the previously reported low density of CTCF occupancy in the *Igκ* locus (Degner et al., 2009), we found ~60 CTCF-binding sites, which were not evenly distributed throughout the *Igκ* locus. We identified five regions with a high density of CTCF sites (regions H1–H5, Figure 6A), and four regions of 150–250 kb with low CTCF occupancy (regions L1–L4, Figure 6A). These four regions, including the proximal region containing V_κ3-family segments (L4; pos. 0 to −250 kb), contained 29 V_κ gene segments, which were rarely used in WT mice (only 1/35 nonproductive alleles). In contrast, regions H2 and H3 contain V_κ gene segments that were frequently used in WT mice (Figure 6B).

Because in the *Igh* locus proximal V_H segments are frequently associated with nearby CTCF sites (Lucas et al., 2011), we examined CTCF occupancy and V_κ segment localization. We found that 26 of the ~60 CTCF sites were located near (<5 kb) a V_κ gene segment (Figure 6A). V_κ gene segments with nearby CTCF sites were mainly present in the proximal half of the *Igκ* locus and were more often used in CTCF WT (9/35) than in CTCF KO (1/41) nonproductive rearrangements.

In summary, we identified ~60 CTCF-binding sites in the *Igκ* locus in pre-B cells. Four regions of 150–250 kb, including the most proximal V_κ region, lacked CTCF occupancy and V_κ segments in these regions were rarely used in WT Igκ alleles.

Loss of CTCF Affects Interactions between the SIS Element and the Proximal Vκ Region

Because of the presence of a predominant CTCF peak at the SIS element, we decided to determine genome-wide interactions mediated by the SIS region in the presence and absence of CTCF, using chromosome conformation capture coupled to high-throughput sequencing (3C-seq) (Soler et al., 2010). To ensure analysis of long-range interactions in non-rearranged Igκ loci, we crossed V_H81X and V_H81X mb1-cre *Ctcf*$^{fl/fl}$ mice on the *Rag1*$^{-/-}$ background. Quantitative RT-PCR analysis of $V_\kappa$germline transcription in sorted B220$^+$CD19$^+$ pre-B cell fractions confirmed that also on the *Rag1*$^{-/-}$ background loss of CTCF was associated with increased germline transcription of

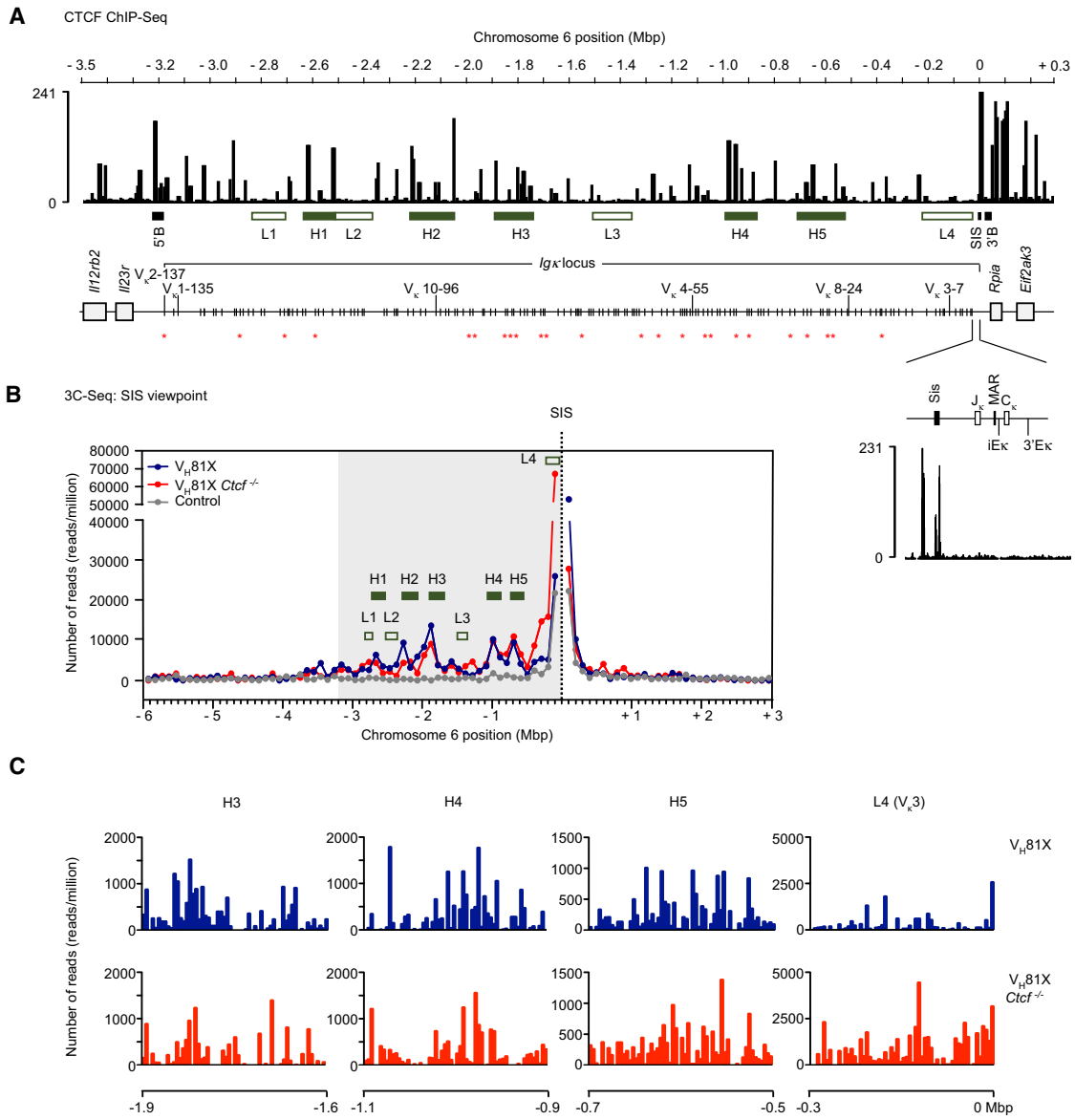

Figure 6. The *Igκ* Locus: Regions with High and Low CTCF Occupancy and the Effects of CTCF Deficiency on Long-Range Chromatin Interactions

(A) Schematic representation of the *Igκ* locus and CTCF-occupancy in pre-B cells, as determined by ChIP-Seq. Strong CTCF sites at the 3′ and 5′boundaries of the locus (5′B and 3′B), as well as within the locus (H1-H5) are indicated. L1-L4 represent regions with low CTCF-occupancy.

(B) 3C-Seq analysis of long-range interactions with the SIS region in B220$^+$CD19$^+$ small pre-B cell populations purified from V_H81X *Rag1*$^{-/-}$ and V_H81X *Rag1*$^{-/-}$ mb1-cre *Ctcf*$^{fl/fl}$ BM and total fetal liver cells. Cross-linked and BglII-digested DNA fragments were ligated and subsequently digested by *NlaIII* followed by re-ligation. Viewpoint-specific primers on the fragment of interest (containing the SIS viewpoint) were used for generating 3C-Seq libraries (see Experimental Procedures for details). The graph shows the number of reads per million in 0.1 Mbp intervals in the 3.2 Mb *Igκ* locus (shaded area) plus 3.0 Mbp upstream and 2.8 Mbp downstream genomic regions. The dashed line represents the viewpoint. 3C-Seq counts obtained for fragments adjacent to the viewpoints were excluded from the analysis.

(C) Number of reads per million obtained for each of the 60 BglII fragments that cover the regions indicated in (B). In each graph, the x axis shows the location in relation to the viewpoint (in Mb). See also Figure S5.

the proximal $V_κ$ gene segment $V_κ$3-7, compared with CTCF-expressing V_H81X *Rag1*$^{-/-}$ pre-B cells (Figure S6). We purified B220$^+$CD19$^+$ pre-B cell populations from control and CTCF-deficient V_H81X *Rag1*$^{-/-}$ BM and performed 3C-Seq experiments, whereby we included E13.5 fetal liver cells as controls. To facilitate direct comparison with $V_κ$ gene usage, we calculated the number of interactions for 100 kb intervals within the *Igκ* locus. Figure 6B shows the long-range interactions identified within a 9 Mb region encompassing the *Igκ* locus and its flanking regions.

In V_H81X *Rag1*$^{-/-}$ small pre-B cells, the SIS element showed interactions throughout the *Igκ* locus, also with regions located at considerable distance (~-3.2 Mbp). Major interactions were found with regions H1–H5, for which we observed high CTCF occupancy. On the other hand, signals were low for the regions L1–L4, where CTCF occupancy was low. In contrast, in non-rearranging control fetal liver cells genomic contacts were reduced to background levels throughout the *Igκ locus* (Figure 6B).

Importantly, when we analyzed CTCF-deficient V_H81X transgenic *Rag1*$^{-/-}$ pre-B cells, we found that the interactions between the SIS region and most of the *Igκ* locus were not different from those identified in CTCF-expressing pre-B cells. Only at the proximal V_κ region (0–300 kb, containing the L4 region) did the SIS region manifest significantly increased interactions (Figure 6B), consistent with increased V_κ usage in the absence of CTCF. Detailed views of V_κ regions with high levels of interaction (H3 and H4) and of the proximal L4 region are shown in Figure 6C.

In summary, these findings demonstrate long-range interactions between the SIS-region and the entire *Igκ* locus, whereby regions with high numbers of identified contacts correlate with the localization of prominent CTCF-binding sites. Nevertheless, the long-range interactions in pre-B cells between the SIS and V_κ region were not notably affected by loss of CTCF; only in the proximal V_κ region did the loss of CTCF result in significantly increased interactions.

CTCF Restricts the Activity of the Enhancer Elements in the *Igκ* Locus

CTCF is thought to function in spatial organization of chromatin topology via loop formation, whereby the positioning of CTCF-binding sites with respect to genes and regulatory elements dictates the types of CTCF-based chromatin loop structures formed (Phillips and Corces, 2009). As a result, CTCF-mediated contacts may either confer enhancer blocking or may enable promoter-enhancer interactions. In rearranged and actively transcribed *Igκ* alleles, long-range interactions between active V_κ gene promoters and the intronic and 3′ enhancers (iEκ and 3′Eκ) are essential for V_κ-J_κ recombination (Liu and Garrard, 2005). Therefore, we next investigated whether CTCF-mediated looping controlled V_κ-J_κ recombination by regulating the spatial proximity of V_κ gene segments relative to the *Igκ* enhancer elements.

In 3C-seq experiments using the iEκ and 3′Eκ enhancers as viewpoints, the identified interactions in the *Igκ* locus paralleled those found for the SIS region, with clear peaks at the H1–H5 regions (Figures 7A and 7B). Although many long-range interactions were preserved in the absence of CTCF, we observed an altered distribution of enhancer contacts: increased interactions with the most proximal part of the V_κ region (H4 and H5 and particularly L4; detailed analyses in Figures 7C and 7D) and decreased distal interactions. In particular, 3′Eκ contacts near the 5′ boundary region, containing the two most distal V_κ genes (V_κ2-137 and V_κ1-135) often used in control (~20%, Figure 4B) but not in CTCF-deficient (pre-)B cells, were reduced (Figures 7B and 7D).

Loss of CTCF also changed interaction of the κ enhancers with regions outside the *Igκ* locus. Beyond the 5′ boundary of the Igκ locus, loss of CTCF was associated with increased iEκ interactions at −4.2 Mbp (region O1) as well as with reduced interactions at −3.7 Mbp (region O2) (Figures 7A and 7C). A large region of ~0.8 Mb, located downstream the 3′ boundary of the Igκ locus (region O3) showed high amounts of interaction with the κ enhancers in CTCF-deficient pre-B cells (Figures 7A, 7B and 7D).

Finally, to exclude the possibility that the observed interactions in our 3C-Seq experiments were affected by the absence of focal Rag1 binding to the J_κ region (Ji et al., 2010), we also performed 3C-Seq experiments for the iEκ and 3′Eκ enhancer viewpoints in sorted pre-B cells from V_H81X and V_H81X mb1-cre *Ctcf*$^{fl/fl}$ mice that were on a Rag1-proficient background. In these analyses, we also found that in the absence of CTCF contacts between the enhancers and the proximal V_κ region or regions outside the Igκ locus were increased (Figure S6).

Taken together, these 3C-seq analyses revealed that interaction between the SIS, Eκ, and 3′Eκ elements and the *Igκ* V region did not require CTCF per se. The absence of CTCF significantly increased the interactions between the enhancer elements and the proximal V_κ region and regions outside the *Igκ* locus.

DISCUSSION

In this study, we used conditional *Ctcf* gene targeting to investigate the function of CTCF during B cell development in vivo. We found that CTCF was critical at the pre-B cell developmental checkpoint, probably as a regulator of genes involved in proliferation and cellular differentiation, but V(D)J recombination still occurred when the *Ctcf* gene was deleted. We studied the *Igκ* locus in detail and found that loss of CTCF resulted in (1) increased proximal V_κ and reduced J_κ germline transcription, (2) increased recombination to proximal V_κ genes, (3) decreased usage of more distal V_κ genes, particularly of the two most distal V_κ genes, and (4) increased interactions of the iEκ and 3′Eκ enhancers with the proximal V_κ region and with elements outside the *Igκ* locus. Our 3C-seq experiments revealed that long-range interactions between the SIS silencer, iEκ or 3′Eκ elements and the *Igκ* V region did not require CTCF per se. Rather, we conclude that CTCF is required for the specificity of interactions between these regulatory elements and V_κ segments, thereby restricting *Igκ* enhancer activity and controlling V_κ gene segment choice.

We demonstrated that in CTCF-deficient pre-B cells proximal V_κ genes are preferentially used for recombination, consistent with increased germline transcription and increased iEκ and/or 3′Eκ enhancer interactions with the V_κ proximal region. In contrast, germline $\kappa^0$0.8/1.1 transcripts, initiated from promoters located upstream of J_κ, were considerably reduced. On the basis of CTCF occupancy in the *Igκ* locus and the observed long-range interactions in the presence and absence of CTCF, we propose a model (Figure S6). In this model, CTCF activity regulates *Igκ* locus recombination by orchestrating functional communications between V_κ gene segments and enhancers, while limiting the actions of *Igκ* locus specific *cis*- and *trans*-acting factors elsewhere in the genome. Strong CTCF-binding sites flanking the *Igκ* locus and in the SIS element in the V_κ-J_κ intergenic region (Degner et al., 2009) would partition off the locus into three main chromatin loop domains, separating the J_κ-C_κ cluster containing the iEκ-3′Eκ enhancers, the proximal part of the V_κ region (with

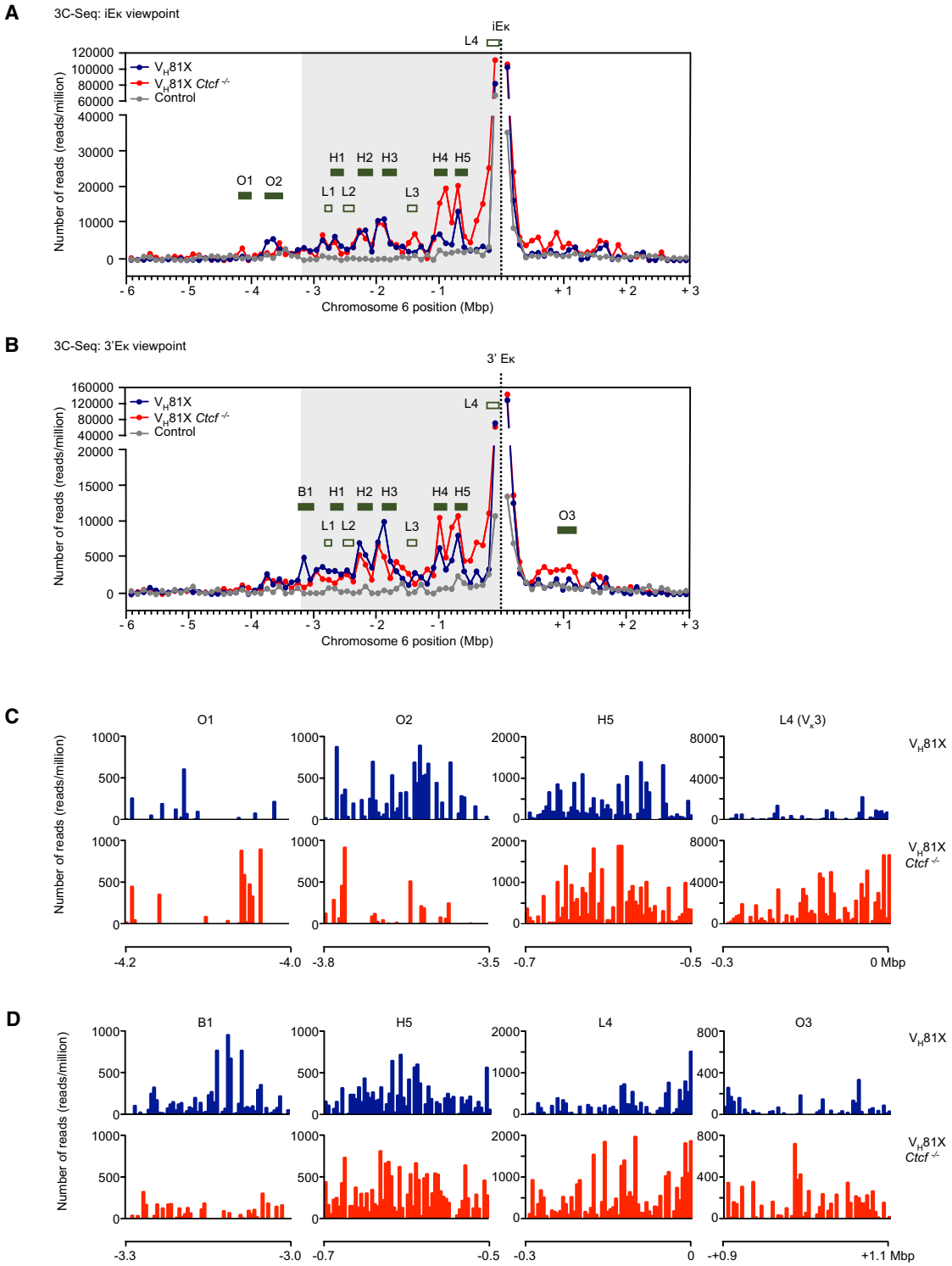

Figure 7. CTCF Restricts Intronic and 3′ κ Enhancer Interactions to the Igκ Light Chain Locus

(A and B) 3C-Seq analysis of long-range interactions with the iEκ (A) or 3′Eκ (B) region in B220^{+}CD19^{+} small pre-B cell populations purified from V_H81X *Rag1*$^{-/-}$ and V_H81X *Rag1*$^{-/-}$ mb1-cre *Ctcf*$^{fl/fl}$ BM and total fetal liver cells. See legend to Figure 6 and Experimental Procedures for details. The graph shows the number of reads per million in 0.1 Mbp intervals in the 3.2 Mb *Igκ* locus (shaded area) plus 3.0 Mbp upstream and 2.8 Mbp downstream genomic regions. The dashed line represents the viewpoint. 3C-Seq counts obtained for fragments adjacent to the viewpoints were not considered.

(C and D) Number of reads per million obtained for each of the 60 BglII fragments that cover the regions indicated in (A) and (B). In each graph, the x axis shows the location in relation to the viewpoint (in Mb). See also Figure S6.

only $V_\kappa 3$ family segments) and the remaining central and distal parts of the V_κ region. Hence, CTCF would prevent inappropriate communication between the *Igκ* enhancers and the promoters of proximal $V_\kappa 3$ gene segments or genomic regions outside the Igκ locus. On the basis of our 3C-Seq experiments showing that in the absence of CTCF most of the long-range interactions within the Igκ locus were conserved, we propose that loss of CTCF has limited effects on the global architecture of the Igκ locus, except for the $V_\kappa 3$ region and the very distal V region containing $V_\kappa 2$-137 and $V_\kappa 1$-135 (Figure S6). CTCF-dependent chromatin looping of the J_κ-C_κ cluster and the iEκ/3′Eκ enhancers would also restrict $V_\kappa 3$ transcription and ensure proper J_κ germline transcription. Consistent with this, deletion of the SIS element results in reduced levels of $\kappa^0$0.8/1.1 germline transcripts (Liu et al., 2006). Very recently, it was shown that mice possessing a 3.7 kb targeted deletion of the SIS element, associated with reduced occupancy of Ikaros and CTCF, display enhanced proximal V_κ usage (Xiang et al., 2011). Increased proximal V_κ usage resulting from loss of CTCF can therefore be attributed to the CTCF sites present in the SIS element.

In our model, dynamic scanning of the V_κ region for recombination would depend on further regulatory sub-loops bringing V_κ gene segments into close spatial proximity with the J_κ-C_κ cluster containing the iEκ-3′Eκ enhancers. Interestingly, recent data demonstrate that the highly active chromatin region encompassing the J_κ segments exhibits focal RAG protein binding (Ji et al., 2010). In this region, V_κ gene segments compete for capture by RAG proteins and therefore it is referred to as a recombination center (Ji et al., 2010). Our finding that long-range interactions between SIS or enhancer elements were most prominent in parts of the *Igκ* locus with strong CTCF-binding sites suggest a function of CTCF in the control of the positioning of V_κ segments relative to the J_κ-C_κ-enhancer region. However, we demonstrated that iEκ-3′Eκ-mediated interactions and recombination to distal V_κ regions can occur in the absence of CTCF, strongly suggesting that CTCF is largely dispensable for *Igκ* locus sub-loop formation. It is conceivable that CTCF cooperates in a redundant fashion with lineage-specific factors bound to the κ enhancers (such as E2A, Pax5 or IRF4) for cell-specific regulation of chromatin looping, as previously demonstrated in Th1 cells (Sekimata et al., 2009). CTCF could alternatively function to direct local histone modifications at the *Igκ* locus (Splinter et al., 2006), and thereby target RAG protein binding. In this context, CTCF may function to epigenetically mark the *Igκ* locus in specific regions at early stages, after which it is no longer essential for the actual recombination process. Nevertheless, in this model loss of CTCF increases contacts between the J_κ-C_κ-enhancer region and $V_\kappa 3$ elements, leading to altered recombination events and inappropriate proximal V_κ usage (Figure S6).

Our data demonstrating that CTCF is not essential for enhancer contacts with the majority of V_κ gene segments is consistent with our previous findings suggesting that CTCF is not absolutely required for TCR-α or TCR-β chain rearrangement in thymocytes (Heath et al., 2008). However, for the *Igh* chain locus a role for CTCF as a regulator of V(D)J rearrangement through the establishment of higher-order chromatin structures has been hypothesized (Degner et al., 2011; Lucas et al., 2011; Ebert et al., 2011). This would be supported by several lines of evidence. First, shRNA-mediated CTCF knockdown increases D_H antisense transcription and decreases *Igh* locus compaction and interactions between D_H and the 3′ regulatory region (Degner et al., 2011). Second, CTCF binds to PAIR elements, which are characterized by Pax5-dependent active chromatin, in the distal V_H cluster in pro-B cells (Ebert et al., 2011) and to many proximal V_H segments, remarkably within 200 bp of their RSS sequences (Lucas et al., 2011). Third, CTCF-binding DNase I-hypersensitive sites within the V_H-D_H intergenic region influence antisense transcription and lineage-specific V(D)J recombination (Featherstone et al., 2010; Giallourakis et al., 2010). However, our findings would not support a model in which CTCF is essential for V(D)J rearrangement, like previously shown for Pax5, Ikaros, or YY1 (Fuxa et al., 2004; Liu et al., 2007; Reynaud et al., 2008). Previous studies have established that conformational changes in *Igh* locus topology that localize V_H regions within close proximity of DJ_H elements occur in committed pro-B cells (Jhunjhunwala et al., 2008). Upon virtually complete deletion of CTCF protein at the pro-B cell stage in the mb1-cre *Ctcf*$^{fl/fl}$ mice, pre-B cells with productive *Igh* rearrangements were still generated. Nevertheless, our finding that the introduction of a pre-rearranged Ig H chain transgene partially rescued differentiation of CTCF-deficient pro-B cells would suggest that loss of CTCF reduces the efficiency of Igh chain recombination. Although both proximal and distal V_H segments can be used in the absence of CTCF, it still remains possible that CTCF is required for efficient recombination to particular V_H segments. Furthermore, we cannot formally exclude that even very low levels of CTCF proteins are sufficient to occupy critical sites in the *Igh* locus at the time of initiation of V(D)J recombination. It is also conceivable that CTCF determines the establishment of a higher-order chromatin structure at early stages in B lymphocyte specification, before the pro-B cell stage, when mb1-cre mediated *Ctcf* gene deletion is not complete. This would be supported by the recent finding that CTCF and E2A already bind to the PAIR elements in *Pax5*$^{-/-}$ pro-B cells prior to *Igh* locus contraction (Ebert et al., 2011). Because CTCF has the ability to influence histone modifications (Splinter et al., 2006), further experiments are required to investigate whether CTCF functions to epigenetically mark the *Igh* locus and thereby control *Igh* looping in lymphoid progenitors.

In summary, our study identifies a role for CTCF in directing functional communications between Igκ enhancers and V_κ promoters in the *Igκ* locus, thereby regulating V_κ gene segment repertoire and restricting the activity of the strong iEκ-3′Eκ enhancers to the *Igκ* locus.

EXPERIMENTAL PROCEDURES

Mice

Ctcf floxed mice (*Ctcf*$^{fl/fl}$; C57BL/6) (Heath et al., 2008) and *Rag1*$^{-/-}$ (Mombaerts et al., 1992), Eμ-Bcl2 (Strasser et al., 1991), μMT (Kitamura et al., 1991), and V_H81X (Martin et al., 1997) mice have been described previously. Mice were bred and maintained in the Erasmus MC animal care facility under specific pathogen-free conditions and were used at 6–13 weeks of age. Experimental procedures were reviewed and approved by the Erasmus University committee of animal experiments.

Flow Cytometry

Preparation of single-cell suspensions, monoclonal antibodies (mAbs) incubations, fluorescein di-β-D-galactopyranoside loading, in vivo BrdU-labeling, and cell cycle analysis have been previously described (Heath et al., 2008;

Middendorp et al., 2002; Ribeiro de Almeida et al., 2009). See Supplemental Experimental Procedures for monoclonal antibodies.

Quantitative RT-PCR Analysis

Total RNA was extracted with the GeneElute mammalian total RNA miniprep system (Sigma-Aldrich) and reverse-transcribed with SuperScript II reverse transcriptase (Invitrogen). For cDNA amplification, Maxima Probe/ROX or SYBR Green/ROX qPCR MasterMix (Fermentas) were used. Primers were designed with the ProbeFinder software (Roche Applied Science) and probes were from the Universal ProbeLibrary (Roche Applied Science) or designed manually (Gapdh) and purchased from Eurogentec (See Supplemental Experimental Procedures). Triplicate reactions were done for each cDNA sample. Gene expression was analyzed with an ABI Prism 7300 Sequence Detector and ABI Prism Sequence Detection Software version 1.4 (Applied Biosystems). Cycle-threshold levels were calculated for each gene and normalized to values obtained for the endogenous reference gene Gapdh. For assessment of the purity of the amplified products, standard agarose gel electrophoresis or melting curve analysis were performed.

Immunoblot Analysis

Nuclear extracts were prepared as previously described (Ribeiro de Almeida et al., 2009). In brief, cytoplasmic proteins were extracted on ice for 10 min (in 10 mM/HEPES-KOH [pH = 7.9], 1.5 mM/$MgCl_2$, 10 mM/KCl, 0.5 mM/DTT, 0.2 mM/PMSF). High-salt extraction of nuclear proteins was carried out on ice for 5 min (in 20 mM/HEPES-KOH [pH = 7.9], 25%/glycerol, 420 mM/NaCl, 1.5 mM/$MgCl_2$, 0.2 mM/EDTA, 0.5 mM/DTT, 0.2 mM/PMSF), followed by centrifugation for removal of cellular debris. Blots were probed with anti-CTCF (1:1500, Upstate), anti-Lsd1 (1:2000, Abcam) as an internal loading control, and the secondary antibody swine anti-rabbit-HRP (1:3000, Dako). Primary Ab incubation was done overnight at 4°C in TBS containing 3% nonfat dry milk and 0.05% Tween-20. Signal detection was performed with ECL (Amersham Biosciences).

DNA Microarray Analysis

Biotin-labeled cRNA was hybridized to the Mouse Gene 1.0 ST Array (Affymetrix). Data were analyzed with the BRB-ArrayTools version 3.7.0 software (National Cancer Institute) with Affymetrix CEL files obtained from GCOS (Affymetrix). The RMA approach was used for normalization. Thresholds for selecting important genes were set at a relative difference > 1.75. Changes in gene expression patterns for mb1-cre $Ctcf^{fl/fl}$ versus WT pro-/pre-B cells were evaluated with Student's t test (with random variance model) and were considered significant with $p < 0.001$. Quantitative RT-PCR was performed on selected genes identified by the microarray analysis to verify their expression levels.

V_κ Gene Sequencing, ChIP Sequencing, and 3C Sequencing

See Supplemental Experimental Procedures in the Supplemental Information for details of V_κ gene usage analysis, ChIP-sequencing, and 3C-sequencing.

Statistical Analysis

To analyze statistical significance, we used a two-tailed Student's t test. p values < 0.05 were considered significant.

SUPPLEMENTAL INFORMATION

Supplemental Information includes six figures, two tables, and Supplemental Experimental Procedures and can be found with this article online at doi:10.1016/j.immuni.2011.07.014.

ACKNOWLEDGMENTS

We thank E. Hobeika and M. Reth (Max Planck Institute for Immunobiology, Freiburg, Germany) for kindly providing mb1-Cre mice, Z. Özgür, C.E.M. Kockx (Biomics, Erasmus MC), and M. Pescatori (Bioinformatics, Erasmus MC) for assistance on Affymetrix microarray analysis and Illumina sequencing, T. Langerak (Immunology) for facilitating DNA sequencing, and the Erasmus MC animal care facility staff. This work was partly supported by Fundação para a Ciência e a Tecnologia (C. R. A.), Dutch Cancer Foundation (KWF, R.W.H.), Royal Netherlands Academy of Arts and Sciences (KNAW, R.S.), the Center of Biomedical Genetics and the EuTRACC Consortium (F.G., E.S. and R. S.).

Received: June 24, 2010
Revised: June 30, 2011
Accepted: July 27, 2011
Published online: October 13, 2011

REFERENCES

Degner, S.C., Wong, T.P., Jankevicius, G., and Feeney, A.J. (2009). Cutting edge: Developmental stage-specific recruitment of cohesin to CTCF sites throughout immunoglobulin loci during B lymphocyte development. J. Immunol. *182*, 44–48.

Degner, S.C., Verma-Gaur, J., Wong, T.P., Bossen, C., Iverson, G.M., Torkamani, A., Vettermann, C., Lin, Y.C., Ju, Z., Schulz, D., et al. (2011). CCCTC-binding factor (CTCF) and cohesin influence the genomic architecture of the Igh locus and antisense transcription in pro-B cells. Proc. Natl. Acad. Sci. USA *108*, 9566–9571.

Düber, S., Engel, H., Rolink, A., Kretschmer, K., and Weiss, S. (2003). Germline transcripts of immunoglobulin light chain variable regions are structurally diverse and differentially expressed. Mol. Immunol. *40*, 509–516.

Ebert, A., McManus, S., Tagoh, H., Medvedovic, J., Salvagiotto, G., Novatchkova, M., Tamir, I., Sommer, A., Jaritz, M., and Busslinger, M. (2011). The distal V(H) gene cluster of the Igh locus contains distinct regulatory elements with Pax5 transcription factor-dependent activity in pro-B cells. Immunity *34*, 175–187.

Engel, H., Rolink, A., and Weiss, S. (1999). B cells are programmed to activate kappa and lambda for rearrangement at consecutive developmental stages. Eur. J. Immunol. *29*, 2167–2176.

Featherstone, K., Wood, A.L., Bowen, A.J., and Corcoran, A.E. (2010). The mouse immunoglobulin heavy chain V-D intergenic sequence contains insulators that may regulate ordered V(D)J recombination. J. Biol. Chem. *285*, 9327–9338.

Fuxa, M., Skok, J., Souabni, A., Salvagiotto, G., Roldan, E., and Busslinger, M. (2004). Pax5 induces V-to-DJ rearrangements and locus contraction of the immunoglobulin heavy-chain gene. Genes Dev. *18*, 411–422.

Giallourakis, C.C., Franklin, A., Guo, C., Cheng, H.L., Yoon, H.S., Gallagher, M., Perlot, T., Andzelm, M., Murphy, A.J., Macdonald, L.E., et al. (2010). Elements between the IgH variable (V) and diversity (D) clusters influence antisense transcription and lineage-specific V(D)J recombination. Proc. Natl. Acad. Sci. USA *107*, 22207–22212.

Grawunder, U., Rolink, A., and Melchers, F. (1995). Induction of sterile transcription from the kappa L chain gene locus in V(D)J recombinase-deficient progenitor B cells. Int. Immunol. *7*, 1915–1925.

Hardy, R.R., Carmack, C.E., Shinton, S.A., Kemp, J.D., and Hayakawa, K. (1991). Resolution and characterization of pro-B and pre-pro-B cell stages in normal mouse bone marrow. J. Exp. Med. *173*, 1213–1225.

Heath, H., Ribeiro de Almeida, C., Sleutels, F., Dingjan, G., van de Nobelen, S., Jonkers, I., Ling, K.W., Gribnau, J., Renkawitz, R., Grosveld, F., et al. (2008). CTCF regulates cell cycle progression of alphabeta T cells in the thymus. EMBO J. *27*, 2839–2850.

Hendriks, R.W., and Middendorp, S. (2004). The pre-BCR checkpoint as a cell-autonomous proliferation switch. Trends Immunol. *25*, 249–256.

Herzog, S., Reth, M., and Jumaa, H. (2009). Regulation of B-cell proliferation and differentiation by pre-B-cell receptor signalling. Nat. Rev. Immunol. *9*, 195–205.

Hobeika, E., Thiemann, S., Storch, B., Jumaa, H., Nielsen, P.J., Pelanda, R., and Reth, M. (2006). Testing gene function early in the B cell lineage in mb1-cre mice. Proc. Natl. Acad. Sci. USA *103*, 13789–13794.

Inlay, M.A., Lin, T., Gao, H.H., and Xu, Y. (2006). Critical roles of the immunoglobulin intronic enhancers in maintaining the sequential rearrangement of IgH and Igk loci. J. Exp. Med. *203*, 1721–1732.

Jhunjhunwala, S., van Zelm, M.C., Peak, M.M., Cutchin, S., Riblet, R., van Dongen, J.J., Grosveld, F.G., Knoch, T.A., and Murre, C. (2008). The 3D structure of the immunoglobulin heavy-chain locus: Implications for long-range genomic interactions. Cell *133*, 265–279.

Jhunjhunwala, S., van Zelm, M.C., Peak, M.M., and Murre, C. (2009). Chromatin architecture and the generation of antigen receptor diversity. Cell *138*, 435–448.

Ji, Y., Resch, W., Corbett, E., Yamane, A., Casellas, R., and Schatz, D.G. (2010). The in vivo pattern of binding of RAG1 and RAG2 to antigen receptor loci. Cell *141*, 419–431.

Jung, D., and Alt, F.W. (2004). Unraveling V(D)J recombination; insights into gene regulation. Cell *116*, 299–311.

Kitamura, D., Roes, J., Kühn, R., and Rajewsky, K. (1991). A B cell-deficient mouse by targeted disruption of the membrane exon of the immunoglobulin mu chain gene. Nature *350*, 423–426.

Liu, Z., and Garrard, W.T. (2005). Long-range interactions between three transcriptional enhancers, active Vkappa gene promoters, and a 3′ boundary sequence spanning 46 kilobases. Mol. Cell. Biol. *25*, 3220–3231.

Liu, Z., Widlak, P., Zou, Y., Xiao, F., Oh, M., Li, S., Chang, M.Y., Shay, J.W., and Garrard, W.T. (2006). A recombination silencer that specifies heterochromatin positioning and ikaros association in the immunoglobulin kappa locus. Immunity *24*, 405–415.

Liu, H., Schmidt-Supprian, M., Shi, Y., Hobeika, E., Barteneva, N., Jumaa, H., Pelanda, R., Reth, M., Skok, J., Rajewsky, K., and Shi, Y. (2007). Yin Yang 1 is a critical regulator of B-cell development. Genes Dev. *21*, 1179–1189.

Lucas, J.S., Bossen, C., and Murre, C. (2011). Transcription and recombination factories: Common features? Curr. Opin. Cell Biol. *23*, 318–324.

Martin, F., Chen, X., and Kearney, J.F. (1997). Development of VH81X transgene-bearing B cells in fetus and adult: Sites for expansion and deletion in conventional and CD5/B1 cells. Int. Immunol. *9*, 493–505.

Middendorp, S., Dingjan, G.M., and Hendriks, R.W. (2002). Impaired precursor B cell differentiation in Bruton's tyrosine kinase-deficient mice. J. Immunol. *168*, 2695–2703.

Mombaerts, P., Iacomini, J., Johnson, R.S., Herrup, K., Tonegawa, S., and Papaioannou, V.E. (1992). RAG-1-deficient mice have no mature B and T lymphocytes. Cell *68*, 869–877.

Nutt, S.L., and Kee, B.L. (2007). The transcriptional regulation of B cell lineage commitment. Immunity *26*, 715–725.

Phillips, J.E., and Corces, V.G. (2009). CTCF: Master weaver of the genome. Cell *137*, 1194–1211.

Reynaud, D., Demarco, I.A., Reddy, K.L., Schjerven, H., Bertolino, E., Chen, Z., Smale, S.T., Winandy, S., and Singh, H. (2008). Regulation of B cell fate commitment and immunoglobulin heavy-chain gene rearrangements by Ikaros. Nat. Immunol. *9*, 927–936.

Ribeiro de Almeida, C., Heath, H., Krpic, S., Dingjan, G.M., van Hamburg, J.P., Bergen, I., van de Nobelen, S., Sleutels, F., Grosveld, F., Galjart, N., and Hendriks, R.W. (2009). Critical role for the transcription regulator CCCTC-binding factor in the control of Th2 cytokine expression. J. Immunol. *182*, 999–1010.

Schlissel, M.S. (2003). Regulating antigen-receptor gene assembly. Nat. Rev. Immunol. *3*, 890–899.

Schlissel, M.S., and Baltimore, D. (1989). Activation of immunoglobulin kappa gene rearrangement correlates with induction of germline kappa gene transcription. Cell *58*, 1001–1007.

Sekimata, M., Pérez-Melgosa, M., Miller, S.A., Weinmann, A.S., Sabo, P.J., Sandstrom, R., Dorschner, M.O., Stamatoyannopoulos, J.A., and Wilson, C.B. (2009). CCCTC-binding factor and the transcription factor T-bet orchestrate T helper 1 cell-specific structure and function at the interferon-gamma locus. Immunity *31*, 551–564.

Soler, E., Andrieu-Soler, C., de Boer, E., Bryne, J.C., Thongjuea, S., Stadhouders, R., Palstra, R.J., Stevens, M., Kockx, C., van Ijcken, W., et al. (2010). The genome-wide dynamics of the binding of Ldb1 complexes during erythroid differentiation. Genes Dev. *24*, 277–289.

Splinter, E., Heath, H., Kooren, J., Palstra, R.J., Klous, P., Grosveld, F., Galjart, N., and de Laat, W. (2006). CTCF mediates long-range chromatin looping and local histone modification in the beta-globin locus. Genes Dev. *20*, 2349–2354.

Strasser, A., Whittingham, S., Vaux, D.L., Bath, M.L., Adams, J.M., Cory, S., and Harris, A.W. (1991). Enforced BCL2 expression in B-lymphoid cells prolongs antibody responses and elicits autoimmune disease. Proc. Natl. Acad. Sci. USA *88*, 8661–8665.

ten Boekel, E., Melchers, F., and Rolink, A.G. (1997). Changes in the V(H) gene repertoire of developing precursor B lymphocytes in mouse bone marrow mediated by the pre-B cell receptor. Immunity *7*, 357–368.

Xiang, Y., Zhou, X., Hewitt, S.L., Skok, J.A., and Garrard, W.T. (2011). A multifunctional element in the mouse Igκ locus that specifies repertoire and Ig loci subnuclear location. J. Immunol. *186*, 5356–5366.